Unsteady flow through a sharp-edged single-hole orifice placed in a pipe

Anantharaman, V.; Waterson, N.; Nakiboglu, G.; Perçin, Mustafa; van Oudheusden, Bas

Publication date
2016

Document Version
Accepted author manuscript

Published in
Proceedings of the International Workshop on Non-Intrusive Optical Flow Diagnostic

Citation (APA)
Anantharaman, V., Waterson, N., Nakiboglu, G., Perçin, M., & van Oudheusden, B. (2016). Unsteady flow through a sharp-edged single-hole orifice placed in a pipe. In *Proceedings of the International Workshop on Non-Intrusive Optical Flow Diagnostic: Delft, The Netherlands*

Unsteady flow through a sharp-edged single-hole orifice placed in a pipe

Vinod Anantharaman[1], Nicholas Waterson[1], Güneş Nakiboğlu[1], Mustafa Perçin[2], Bas van Oudheusden[2]

[1] *Department of Environment Control & Infrastructure (EC&I), ASML, The Netherlands*
[2] *Department of Aerospace Engineering, Delft University of Technology (TU Delft), The Netherlands.*

1. Introduction

Orifice plates or flow restrictions are key components used in industry for flow measurement and control. They find application in gas and liquid circuits of, e.g., lithography machines, nuclear power plants and aerospace propulsion systems [1]. They are used typically either for measuring flow-rate or to introduce a pressure drop for purposes of flow balancing. It is widely acknowledged in literature that the turbulent, unsteady nature of the flow through an orifice can be a source of structural vibration [2].

2. Experimental Approach

In order to understand the nature of the vibration source, experimental investigations were performed to analyze the time-varying flow field by means of:

- unsteady wall-pressure measurements, see Figure 2; and
- time-resolved, planar, particle-image velocimetry (PIV), see Figure 3;

focusing on the flow behavior downstream of the orifice [3]. All tests were performed with water as the working fluid under fully-developed turbulent flow conditions. The average flow velocity (U_p) in the pipe was varied between 0.5-3.0 m/s giving a Reynolds number range Re_p=4000-27000, based on the pipe diameter (D_p) and U_p. The geometrical parameters characterizing a sharp-edged, single-hole orifice are summarized in Figure 1. Several orifices with varying porosity β and thickness to hole-diameter ratio, t/d_h, were tested.

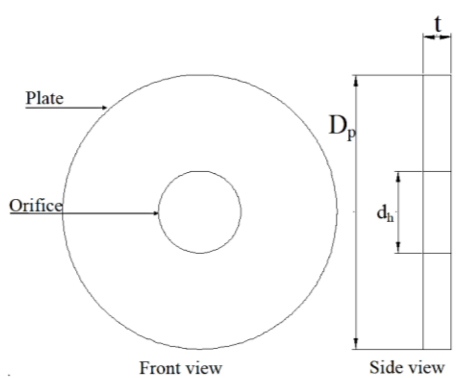

- Pipe diameter, D_p
- Hole diameter, d_h
- Thickness, t
- Thickness to hole-diameter ratio, t/d_h
- Open-area ratio (porosity) $\beta=(d_h/D_p)^2$

Figure 1: Geometry of sharp-edged single-hole orifice and nomenclature

2.1 Unsteady pressure measurements

A continuous flow of water, supplied by a pump, passes through the test section in which the orifice plate is located before returning to the pump reservoir via a flow meter. Pressure sensors are positioned upstream and downstream of the orifice. A differential pressure manometer measures the steady pressure difference between the flow inlet and outlet.

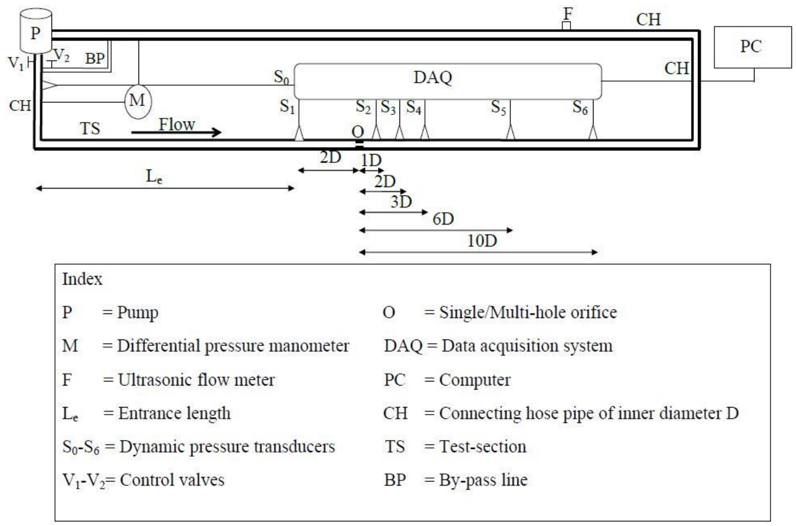

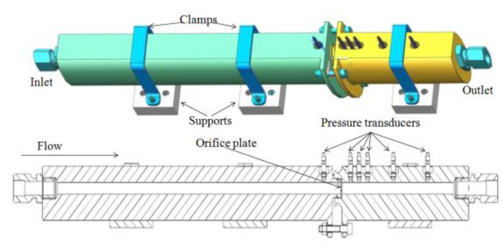

Pressure sensor type	S_1-S_6: PCB 105C02, S_0: KISTLER 7261
Acquisition frequency	2048 Hz
Sampling time	82 sec
Data acquisition system	PAK MKII and PAK 5.8 software

Figure 2: Schematic of the experimental setup used for pressure measurements (left), test section (upper right), summary of data acquisition parameters (lower right).

2.2 Time-resolved planar particle image velocimetry (PIV)

Water containing seeding particles, driven by a pump, passes through a flow meter and settling chamber before approaching the orifice plate under fully-developed turbulent conditions. The fluid issuing from the orifice passes through a transparent glass tube of wall thickness 0.3mm and into an octagonal glass tank. The entire test section is submerged in water inside the octagonal tank and water flow into the tank is carried back to the reservoir.

The measurement region is formed by the two-dimensional central longitudinal plane of the glass pipe downstream of the orifice plate. The particles moving in this plane are illuminated by a light sheet produced by a high-speed laser. To extend the measurement region in the stream wise direction, two high-speed cameras are used, which are positioned on opposite sides of the tank, with a viewing direction orthogonal to both the tank wall and the laser-light sheet. The triggering of the laser illumination and image acquisition by the cameras is synchronized by a high-speed controller.

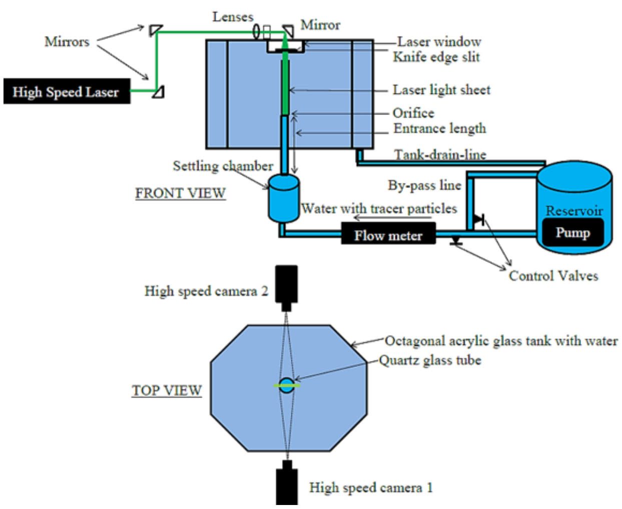

Seeding	Silver coated hollow glass spheres Mean diameter: 10 μm Concentration: 15 particles/mm^3
Illumination	Litron laser Maximum repetition rate: 20kHz Sheet thickness: 0.5 mm
Recording device	High-speed star 6 (Two) Minimum exposure time: 1 μs Maximum repetition rate of 5.4 kHz at 1024×1024 pixels Maximum repetition rate of 12.5 kHz at 384×1024 pixels Pixel pitch: 20 μm
Optical arrangement	Nikon lenses: $f = 180\ mm$ Extension rings: 36, 20 and 16 mm $f_{\#} = 5.6$
Complete image size	Camera-1 = $37 \times 37\ mm^2$ at 27.7 mm/px Camera-2 = $37.8 \times 37.8\ mm^2$ at 27.08 mm/px
Measurement Field of View	Camera-1 = $8.4 \times 32.6\ mm^2$ or $1D \times 3.9D$ Camera-2 = $8.4 \times 37.8\ mm^2$ or $1D \times 4.5D$ Overlap region = $2.9D - 3.9D$ Complete flow field = $8.4 \times 62\ mm^2$ or $1D \times 7.4D$
Acquisition frequency	Double frame at 1.5 kHz Single frame at 12.5 kHz
Number of images	Double frame: 3000 images in 2 s Single frame: 6000 images in 480 ms

Figure 3: Schematic of the experimental setup used for time-resolved planar PIV measurements (left); summary of measurement conditions (right).

3. Results and Discussion

The measurements provide detailed insights into the flow behavior downstream of orifice plates and some of the key observations are described below. In all figures the flow direction is from left to right. Axial (streamwise) distances, x, are specified with respect to the orifice exit (x=0) and the radial distances, y, are specified with respect to one side of the pipe.

3.1 Unsteady flow field

Some of the time-varying features of the orifice jet can be seen in Figure 4. The jet length is observed to vary in time. It appears that the shear layer grows (extend) till a certain extent after which a portion of the fluid breaks-off upon which the jet length decreases again. Another noticeable feature is the constriction of the jet. These images also illustrate the lateral motion of the jet with respect to the pipe centerline, which appears as a flapping motion in the time series.

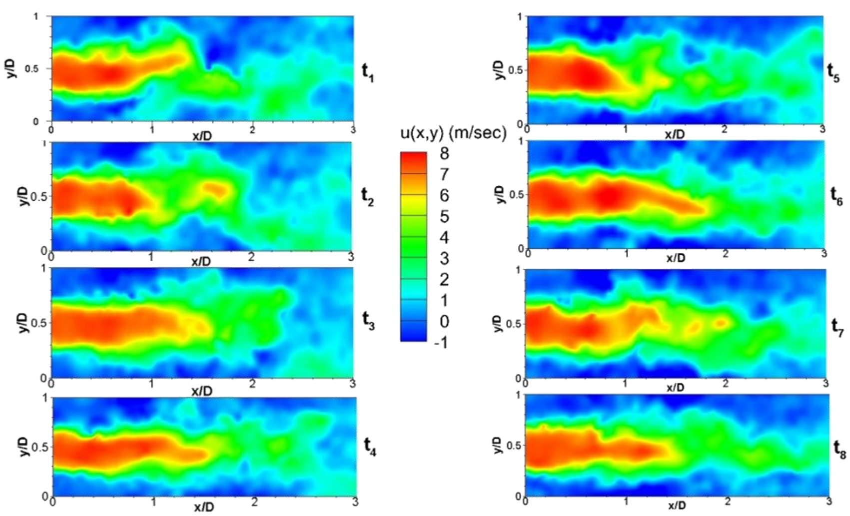

Images show the instantaneous flow-field at a series of time instants time instant $\{t_1,t_2\ldots t_8\}$ with each pair separated by 20 images.

Vector fields computed using sliding sum of correlation with ±3 images on data sampled at 12500Hz.

Figure 4: Unsteady flow field downstream of single-hole orifice illustrated by contours of axial velocity with β=20%; t/d_h=0.5, U_p=1m/s (Re_p=8383).

Analysis of the pressure spectra reveals the existence of a dominant frequency close to the orifice (up to x=1-2D_p), see Figure 5, which is observed to scale linearly with the flow velocity in the measurement range.

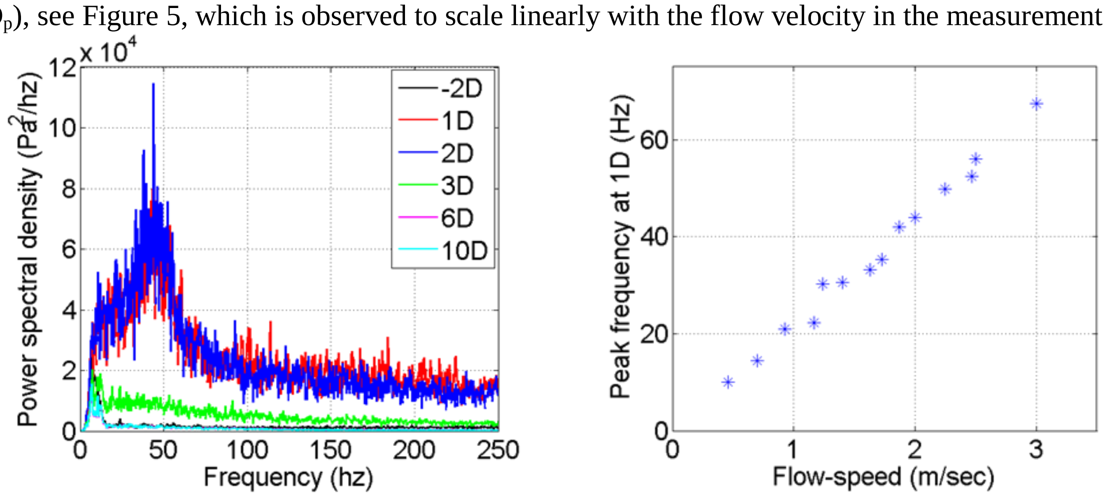

Figure 5: PSD of the pressure spectra for flow through a single-hole orifice with β= 20%, t/d_h=0.5 U_p= 2m/s, Re_p=18000 (left) and variation of the dominant frequency with pipe flow speed (right).

3.2 Advanced flow diagnostics

The spectra of the wall-pressure fluctuation data were compared against velocity field spectra extracted from the temporal mode of a Proper Orthogonal Decomposition (POD) of the PIV data (see Figure 6). The dominant peak in the spectrum agrees well with the pressure data, while the spatial distribution of the POD mode indicates that the primary instability of the orifice jet is a low-frequency flapping motion sustained by the surrounding large recirculation regions.

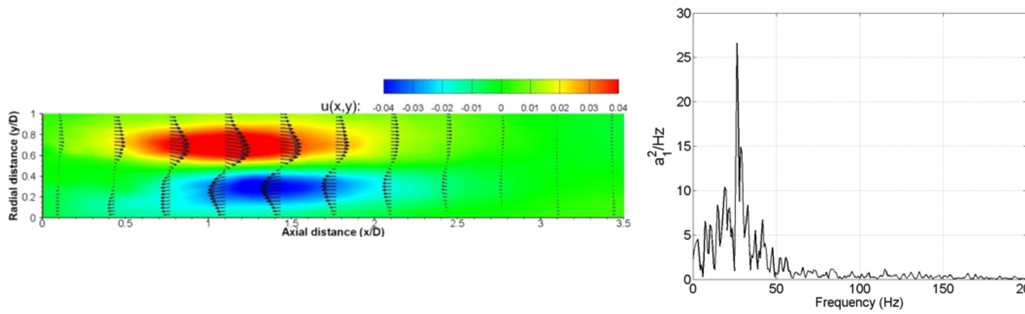

Computed using a data set of 1000 snapshots. U_p=1m/s (Re_p=8383) for an orifice with β=20% and t/d_h=0.5

Figure 6: The first POD spatial mode (left) and the spectrum of the corresponding temporal mode (right)

For the geometries of the sharp-edged single-hole orifices investigated (with t/d_h=0.5), the flapping frequency was observed to increase with the flow speed with a Strouhal number ≈ 0.02 based on the orifice jet velocity and pipe to orifice diameter difference, (D_p – d_h), see Figure 7.

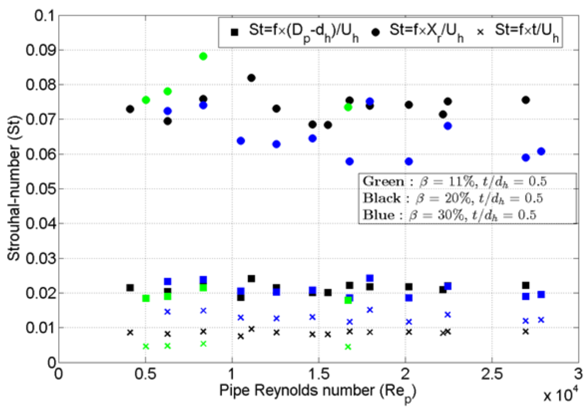

Symbols used are for different length scales, ■ (D_p - d_h), ● re-attachment length X_r and × plate thickness t. Different orifice geometries indicated by color.

Figure 7: Comparison results for different Strouhal number definitions as a function of pipe Reynolds number (Re_p), corresponding to the low-frequency peak obtained from the wall-pressure data.

Reference

[1] V. Ahuja, A. Hosangadi, M. Hitt and D. Lineberry, "Numerical Simulations of Instabilities in Single-Hole Orifice Elements," In 49th AIAA/ASME/SAE/ASEE Joint Propulsion Conference, 2013.

[2] D. S. Weaver, S. Ziada, M. K. Au-Yang, S. S. Chen, M. P. Pa\"{i}doussis and M. J. Pettigrew, "Flow-induced vibrations in power and process plant components-progress and prospects," Journal of Pressure Vessel Technology, vol. 122, pp. 339-348, 2000.

[3] V. Anantharaman, "Characteristics of flow through orifices in pipes: an experimental investigation," TU Delft, 2014.